



Contents lists available at ScienceDirect

## Bioorganic &amp; Medicinal Chemistry

journal homepage: [www.elsevier.com/locate/bmc](http://www.elsevier.com/locate/bmc)

# Synergism of virtual screening and medicinal chemistry: Identification and optimization of allosteric antagonists of metabotropic glutamate receptor 1

Tobias Noeske<sup>a,b</sup>, Dina Trifanova<sup>c</sup>, Valerjans Kauss<sup>c</sup>, Steffen Renner<sup>a</sup>, Christopher G. Parsons<sup>a</sup>, Gisbert Schneider<sup>b,\*</sup>, Tanja Weil<sup>a,d,\*</sup>

<sup>a</sup> Merz Pharmaceuticals GmbH, Altenhöfer Allee 3, D-60438 Frankfurt, Germany

<sup>b</sup> Johann Wolfgang Goethe-University, Institute of Organic Chemistry and Chemical Biology ZAFES/CMP, Siesmayerstraße 70, D-60323 Frankfurt, Germany

<sup>c</sup> Latvian Institute of Organic Synthesis, 21 Aizkraukles, Riga LV 1006, Latvia

<sup>d</sup> National University of Singapore, 3 Science Drive 3, Singapore 117543, Singapore

## ARTICLE INFO

## Article history:

Received 28 November 2008

Revised 27 May 2009

Accepted 28 May 2009

Available online xxxxx

## Keywords:

mGluR1

Metabotropic

Antagonist

Self-organizing map

Virtual screening

## ABSTRACT

We report the identification of novel potent and selective metabotropic glutamate receptor 1 (mGluR1) antagonists by *virtual* screening and subsequent hit optimization. For ligand-based *virtual* screening, molecules were represented by a topological pharmacophore descriptor (CATS-2D) and clustered by a self-organizing map (SOM). The most promising compounds were tested in mGluR1 functional and binding assays. We identified a potent chemotype exhibiting selective antagonistic activity at mGluR1 (functional  $IC_{50} = 0.74 \pm 0.29 \mu M$ ). Hit optimization yielded lead structure **16** with an affinity of  $K_i = 0.024 \pm 0.001 \mu M$  and greater than 1000-fold selectivity for mGluR1 versus mGluR5. Homology-based receptor modelling suggests a binding site compatible with previously reported mutation studies. Our study demonstrates the usefulness of ligand-based *virtual* screening for scaffold-hopping and rapid lead structure identification in early drug discovery projects.

© 2009 Elsevier Ltd. All rights reserved.

## 1. Introduction

G-protein coupled receptors (GPCRs) represent the largest family of cell-surface receptors involved in signal transmission.<sup>1</sup> They are divided into three families displaying distinct differences concerning their sequence similarity and their mechanism of receptor activation: Family 1—for example, rhodopsin/ $\beta$ -adrenergic receptors, family 2—for example, secretin receptors and family 3—for example, metabotropic glutamate receptors (mGluRs).<sup>2</sup> mGluRs have been subdivided into three groups based on sequence identity, signal transduction and pharmacology: Group I consists of mGlu1 and mGlu5, group II comprises mGlu2 and mGlu3, and group III holds mGlu4, 6, 7 and 8.<sup>3</sup> mGluRs are characterized by a large extracellular domain (ECD) containing a Venus flytrap module for orthosteric agonist binding.<sup>4</sup> After agonist binding to the ECD, signal transduction proceeds via the heptahelical domain (HD), which is composed of seven transmembrane helices linked to each other by alternating extracellular and intracellular loops and an intracellular domain (ICD) including the C terminus and the G-protein interaction sites. Allosteric agonists and antagonists

of mGluRs have been found to bind within the HD.<sup>5</sup> The allosteric binding site is considered to have a higher 'druggability' than the orthosteric binding site<sup>6–8</sup> and therefore, several attempts to identify novel allosteric modulators of different mGluRs have been described.<sup>6,9</sup> Negative modulation of mGluR1 has been suggested as a potential therapeutic approach for a variety of indications, for example, different pain states,<sup>3</sup> depression<sup>10</sup> and several forms of cancer.<sup>11</sup> Therefore, there is a vivid interest in the identification of mGluR1 inhibitors suitable for *in vivo* experiments and several potent mGluR1 antagonists have been identified.<sup>12–15</sup> So far, most known mGluR modulators were discovered applying high throughput screening technologies. However, recently several successful attempts applying ligand-based *in silico* approaches for the identification of hit compounds interacting with mGluRs have been reported.<sup>15–17</sup> Ligand-based approaches are fast and allow *virtual* screening of large databases of hundreds of thousands of compounds. Such methods are often based on the concept of molecular similarity that states that molecules with similar features are likely to exhibit similar biological responses.<sup>18,19</sup> Recently, negative allosteric modulators of mGluR1 and mGluR5 have been identified applying ligand-based *virtual* screening methods such as homology model-based virtual screening,<sup>18</sup> alignment-free topological pharmacophore descriptors,<sup>15</sup> neural network ensembles<sup>16</sup> or pharmacophore models<sup>20</sup> that served as valuable starting points for hit optimization approaches.

\* Corresponding authors. Tel.: +49 6979824873; fax: +49 6979824880, tel.: +65 65161377; fax: +65 6779 1691 (T.W.).

E-mail addresses: [G.Schneider@chemie.uni-frankfurt.de](mailto:G.Schneider@chemie.uni-frankfurt.de) (G. Schneider), [chmweilt@nus.edu.sg](mailto:chmweilt@nus.edu.sg) (T. Weil).

In this article, we report the identification of novel selective metabotropic glutamate receptor 1 (mGluR1) antagonists with nanomolar affinities by *virtual* screening and subsequent hit optimization. For ligand-based *virtual* screening, molecules were represented by a topological pharmacophore descriptor (CATS-2D) and clustered by a self-organizing map (SOM). Homology-based receptor modelling suggests a binding site compatible with previously reported mutation studies.<sup>15,20</sup> We have focused the hit optimization process on activity optimization as well as achieving selectivity versus mGluR5, which represents the structurally closest analogue sharing a high sequence identity with mGluR1. mGluR1 antagonists often display limited selectivity versus the mGluR5 receptor<sup>20</sup> and it has been shown that the combined administration of an mGluR1 and an mGluR5 antagonists resulted in the occurrence of more pronounced side-effects.<sup>21</sup> Therefore, selectivity versus the mGluR5 receptors is considered crucial for the development of mGluR1 antagonists. In addition, due to their binding site within the transmembrane domain, the combination of high functional activity and acceptable water-solubility for *in vivo* and *in vitro* studies is an additional key concern.

## 2. Results and discussion

### 2.1. Virtual screening

The self-organizing map (SOM) principle was introduced by Kohonen in 1982,<sup>22</sup> and has been applied to a variety of tasks in chemistry and chemical biology since that time.<sup>23,24</sup> We have recently reported a combination of molecule encoding and clustering to predict compound selectivity,<sup>25</sup> which was realized by a topological pharmacophore descriptor<sup>26</sup> and the SOM algorithm.<sup>27,28</sup> Here we employed this concept for *virtual* screening of a large compound library for potential allosteric mGluR1 antagonists. First, we defined 'drug-like chemical space' using a SOM projection of drug-like compounds.<sup>25</sup> Each molecule was encoded by a 150-dimensional descriptor (CATS-2D)<sup>26</sup> giving scaled frequencies of pairs of potential pharmacophore points (PPP) in the molecular graph. The underlying dataset was the COBRA (v.3.12) collection of pharmacologically active molecules.<sup>27</sup>

The SOM projection is topology-preserving, that is, molecules which are located close to each other on the map, are also adjacent in the original high-dimensional space. Here, a map with either 100 or 225 'neurons' (clusters), each of which contains molecules having certain pharmacophore features in common. In the next step, a subset of 357 reference compounds including 213 published and Merz *in-house* structures of allosteric mGluR1 antagonists was mapped onto the trained SOMs. In both maps we visualized the distribution of the reference molecules (Fig. 1). Considering that these SOMs have a toroidal topology, both of them (10 × 10 and 15 × 15 grid) reveal one large cluster, one smaller cluster and several distributed 'activity islands' containing reference compounds. Neurons 8/7 and 6/6 displayed the highest density of mGluR1 antagonists (Fig. 1a).

Finally, the Asinex Gold Collection 2003 (194,563 compounds) was projected onto the SOMs. Again, the maps were coloured according to compound density (Fig. 1b). Since we were interested in only those Asinex compounds that contain pharmacophoric features similar to known mGluR1 antagonists, we focused on neurons 8/7 and 6/6 exclusively (Fig. 1): Molecules that are co-located are assumed to have similar pharmacological activity.<sup>25,27,28</sup> Neuron 8/7 (10 × 10 map) contained 1864 molecules, and 6/6 (15 × 15 map) contained 749 molecules. All Asinex compounds that were retrieved by both maps were selected and ranked according to their distance to the cluster centroids.

Twenty eight screening candidates were manually selected from the top-ranking 60 compounds based on structural novelty with respect to already known mGluR1 antagonists, ordered and tested in both binding and functional assays. Details on the conduction of the assays were included in Section 4. We obtained a screening result hit rate of >20% at a ligand concentration of 10 μM: One compound was 'highly active' (<1 μM), five compounds (18%) were 'moderately active' (1–15 μM), seven compounds (25%) exhibited 'low activity' (15–40 μM), and for 15 compounds (54%) we observed 'no activity' (>40 μM). Bioactivity data for molecules with propenone as a common structural moiety are given in Table 1. Structures and data of the remaining compounds from this study can be found in the Supplementary data in S-Table 1. Noteworthy, all propenone-derivatives were inactive at rat mGluR5 (rmGluR5).

### 2.2. Structure–activity relationship

Comparing hits **3** and **4** shows a fourfold preference of a 6-methyl substituent over a 7-methyl substituent at the quinoline group. **1** versus **5**—an analogue of **3** but with benzene (**1**) or a *p*-methoxybenzene ring (**5**) instead of the thienyl-substituent—showed a 12-fold deterioration for the addition of a methoxy-group at the *para*-position of the benzene ring. A similar trend is observed comparing **7** containing both unfavourable substituents and **1** leading to a more than 20-times decreased antagonistic activity (Table 1). We tried to explain the interaction of **1** with rmGluR1 by means of our own homology model of rmGluR1 (Fig. 2a) that was published recently.<sup>15,20</sup> The model suggests the presence of three hydrogen-bond donors (R661<sup>3,29</sup>/N747<sup>45,51</sup>, S668<sup>3,36</sup> and T815<sup>7,39</sup>) in the allosteric antagonist binding pocket of mGluR1, flanked by two hydrophobic regions (region I: V753<sup>5,43</sup>, P756<sup>5,46</sup>, V757<sup>5,47</sup>; region II: L640<sup>2,58</sup>, P645<sup>2,63</sup>, V819<sup>7,43</sup>).

Ligand **1** was manually docked into the homology model to best explain the observed structure–activity data, followed by energy minimization within the receptor pocket according to a procedure that has been published recently.<sup>15,20</sup> Since no activity was found in human mGluR1 (hmGluR1) for molecules **1–7** (data not shown), the ligands were also assumed to interact with V757<sup>5,47</sup>, which represents the single amino acid difference between rat and human receptors within the ligand-binding region<sup>15</sup>: V757<sup>5,47</sup> (5.47 according to the numbering scheme of Ballesteros<sup>29</sup>) in rmGluR1 versus L757 in hmGluR1.<sup>15</sup> Another possibility could be that the amino acid species difference led to an alternate conformation of the binding site. Given that many known ligands bind to both species,<sup>15,20</sup> the binding site difference should likely be local around the mutation, and would also justify to place a part of the ligand near to V757<sup>5,47</sup>. The predicted binding mode for **1** is shown in Figure 2.

In the hypothesized binding mode of **1** the ligand interacts with the hydrogen-bonding cluster of R661<sup>3,29</sup> and N747<sup>45,51</sup> via the linker carbonyl oxygen. The quinoline-nitrogen hydrogen-bond acceptor interacts with T815<sup>7,39</sup>. Notably, the linker-conformation orients both potential hydrogen-bonding groups in the same direction, towards the N-terminal domain of the receptor. According to our receptor model, the *para*-methoxy group of the benzene ring of **1** would sterically interfere with the hydrophobic cluster at TM5, in particular with V757<sup>5,47</sup>. At the opposite end of the binding site, a 7-methyl substituent at the quinoline of **1** would interfere with the hydrophobic cluster at TM2, most likely with P645<sup>2,63</sup>.

The predicted binding mode is in agreement with the binding pocket of EM-TBPC<sup>30</sup> (1-Ethyl-2-methyl-6-oxo-4-(1,2,4,5-tetrahydro-benzo[*d*]azepin-3-yl)-1,6-dihydro-pyrimidine-5-carbonitrile) that has been determined by a mutation study.<sup>30</sup> All residues identified to influence ligand binding (V757<sup>5,47</sup>, W798<sup>6,48</sup>, F801<sup>6,51</sup>, Y805<sup>6,55</sup>, T815<sup>7,39</sup>) are in proximity to **1** in our model. N747A<sup>45,51</sup>

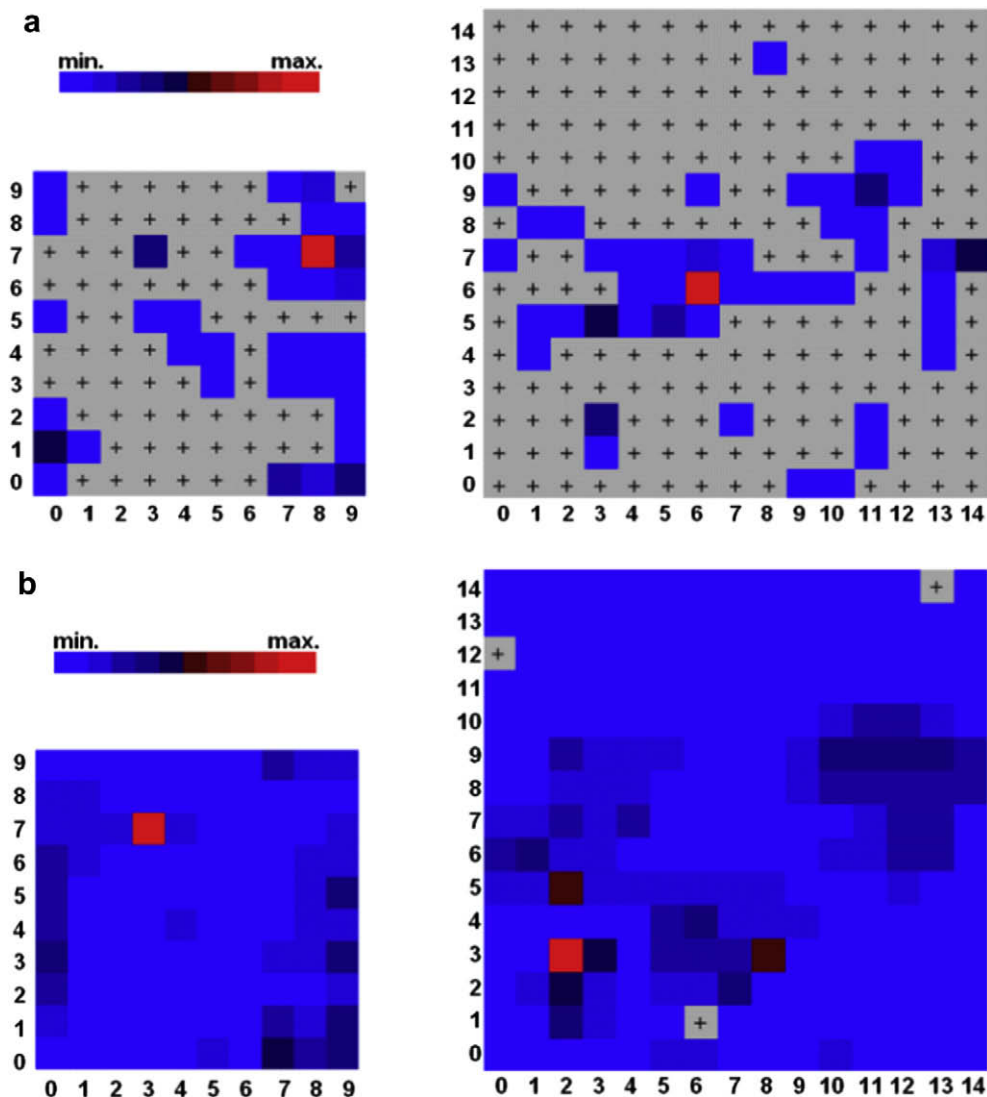


**Figure 1.** Self-organizing map showing the distribution of mGluR1 reference molecules ( $N = 357$ ) (a) and distribution of the candidate screening compounds ( $N = 194,563$ ) (b) in topological pharmacophore space (CATS-2D descriptor). Colouring reflects relative compound density.

was found to increase the activity of EM-TBPC,<sup>30</sup> which is in agreement with the lack of a corresponding hydrogen-bonding partner on that ligand.

### 2.3. Activity optimization via the synthesis of structural analogues

The putative allosteric binding site of rmGluR1 (Fig. 2a and b) reveals several hydrophobic amino acids, for example, V757, V753, V819, L640 and V664. Therefore, the replacement of the phenyl, thiophenyl or furyl substituents of **1–7** by an alkyl or cyclic alkyl group might lead to an improved binding affinity for rmGluR1. Consequently, a small library of alkylpropenone derivatives was synthesized as shown in Scheme 1. The synthesis of alkylpropenone derivatives **8–12** is a one-step reaction based on a condensation reaction of an aldehyde with an alkylketone.<sup>31</sup> Scheme 1 shows the reaction of quinoline-3-carbaldehyde (**17**) with 1-adamantan-1-yl-ethanone (**18**) in the presence of sodium hydroxide to give 1-adamantan-1-yl-3-quinolin-3-yl-propenone (**10**) in high yield. A detailed description of the synthesis of all propenone derivatives **8–12** of Table 2 is given in Section 4.

Since  $\alpha,\beta$  unsaturated ketones are generally known to be good *Michael* acceptors, limited metabolic stability might occur due to an interaction with for example, cysteine groups. Therefore, the vinyl group in **8–12** was converted into a cyclopropyl ketone group, which has similar steric requirements and polarity but lacks the potentially active site for *Michael* addition reactions (Scheme 1). In this way, cyclopropylketones **13–16** were synthesized according to a *Corey–Chaykovsky* reaction where the  $\alpha,\beta$ -unsaturated ketone was reacted with trimethyl sulfoxonium iodide (*Corey–Chaykovsky* reagent), which was generated from dimethylsulfoxide and methyl iodide to give the respective cyclopropyl ketone in good yields.<sup>32,33</sup> A description of the synthesis is given in Section 4.

The attachment of a cyclopropylpropenone group gave **8** displaying no affinity for rmGluR1. However, in case a *tert*butylpropenone group (**9**) was introduced as a substituent, a moderately active rmGluR1 antagonist was gained (Table 2). Highly active rmGluR1 antagonists were obtained after the introduction of a bulky adamantanylpropenone group (**10–17**). Here, antagonist **10** revealed a high affinity for mGluR1 with a  $K_i$  of 0.02  $\mu\text{M}$ . However, a considerable interaction with rmGluR5 was detected ( $K_i$  of 0.807  $\mu\text{M}$ ) thus resulting in only 30-fold selectivity for rmGluR1 versus rmGluR5. It was shown previously that dual inhibition of

**Table 1**  
Structure and in vitro functional ( $IC_{50}$ ) and binding ( $K_i$ ) results for propenone-based screening compounds

Chemical structure	ID	$IC_{50}$ ( $\mu$ M) rmGluR1	$K_i$ ( $\mu$ M) rmGluR1	$K_i$ ( $\mu$ M) rmGluR5
	<b>1</b>	1.7 ( $\pm$ 0.15)	9.18 ( $\pm$ 1.08)	>100
	<b>2</b>	8.5 ( $\pm$ 0.62)	>40	>100
	<b>3</b>	0.74 ( $\pm$ 0.29)	9.93 ( $\pm$ 1.25)	>100
	<b>4</b>	2.97 ( $\pm$ 0.40)	17.23 ( $\pm$ 2.14)	>100
	<b>5</b>	20.5* ( $\pm$ 5.28)	>40	>100
	<b>6</b>	>40	>40	>100
	<b>7</b>	39.30* ( $\pm$ 16.3)	>40	>100

Results are the mean values of at least two independent experiments. Asterisks indicate values were estimated from single concentrations. Standard errors are given in parentheses.

both mGluR1 and mGluR5 leads to more pronounced side effects in vivo, for example, cognitive impairment.<sup>21</sup> Therefore, the reduction of mGluR5 activity is crucial to diminish those side effects. The presence of a 2,3-dihydro-benzo[1,4]dioxine or a 4-methoxy-3-methyl-phenyl group in **11** and **12**, respectively, gave rmGluR1 antagonists with reduced affinities and lower selectivities versus rmGluR5.

It is noteworthy that the conversion of the propenone group of **10** into a cyclopropylketone group (**13–16**) yielded an rmGluR1 antagonist with an improved selectivity profile. Compound **13** was achieved by converting the propenone group of **10** into a cyclopropylketone group resulting in a about sixfold reduction of rmGluR1 binding affinity but no affinity for rmGluR5 up to 10  $\mu$ M. Replacement of the quinoline group of **13** by a pyridyl group (**14**) significantly reduced both the affinity for rmGluR1 and the selectivity versus rmGluR5. In case the pyridyl group carried an *o*-methoxy (**15**) the binding affinity was recovered in combination with an improved selectivity. A superior in vitro profile was achieved after attaching an *o*-morpholino group to the pyridyl ring of **14**. In contrast to all other rmGluR1 antagonists reported herein, **16** combined high affinity for rmGluR1 as well as selectivity versus mGluR5 and an improved water-solubility due to the presence of the morpholino group thus allowing its use for in vivo experiments. In addition, a high affinity for the human mGluR1 receptor (hmGluR1) was gained (Table 2).

The results for the optimized ligands agree well with the propenone binding mode postulated for **1** in our homology model, and with two earlier studies where we predicted binding modes on

the basis of SAR for series of coumarines<sup>15</sup> and tetrahydroquinolones.<sup>20</sup> Within the coumarine series, a carbonyl-linked adamantyl group was predicted to interact with the hydrophobic cluster at TM5, similar to the optimized ligands **10–16**. For the tetrahydroquinolinone series, several ligands were found with piperazine or tetrahydropiperidine substituents that might well overlap with the morpholine group of **16**. The comparable rmGluR1 affinity of **10** and **16** indicates that the tertiary amino group of the morpholine ring is most likely not in a charged state, which is also well in agreement with the predominantly hydrophobic binding site in mGluR1, and in particular with the interaction of the morpholine substituent with the second hydrophobic cluster at TM2 and TM7.

### 3. Conclusion

In a prospective *virtual* screening study, we have compiled a small subset from a large and diverse compound library yielding a substantial hit rate. Some molecules showed functional activity at rmGluR1 at the low micromolar and even nanomolar level. Economic chemical optimization resulted in potent and selective lead candidates. The tight interplay of *virtual* screening and medicinal chemistry was a key to success.

Based on pharmacological results, we hypothesize a binding mode for the propenone hits, that was well in agreement with mutational data on other mGluR1 ligands.<sup>30</sup> Knowledge of a potential binding site facilitated the design of novel mGluR1 antagonists

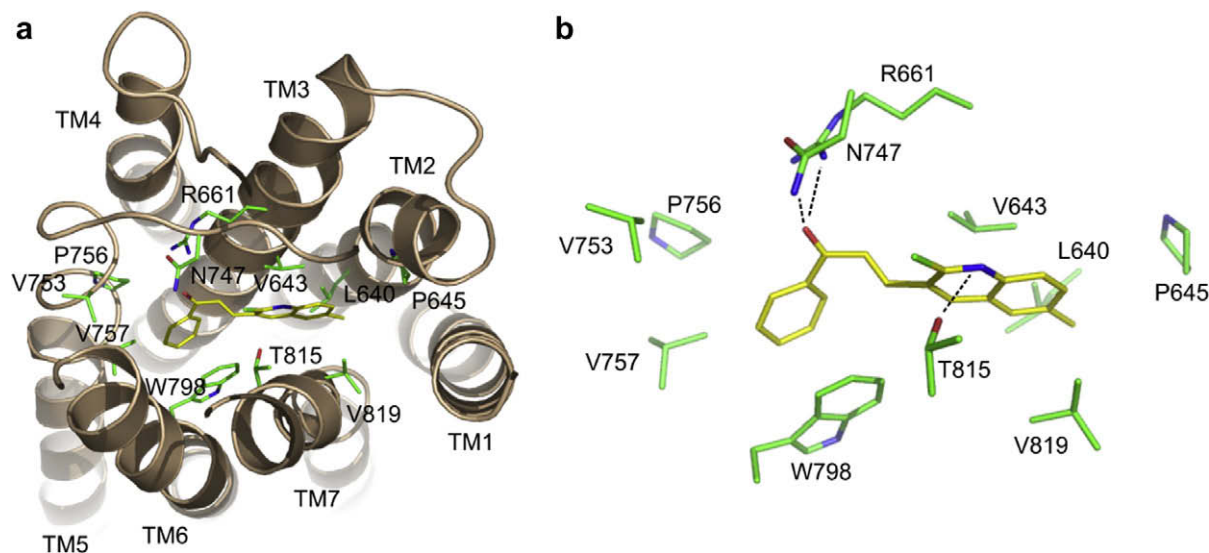


**Figure 2.** Potential binding mode of **1** in the allosteric binding site of rmGluR1; (a) overview, (b) detailed view.

with a markedly improved activity and selectivity profile. In particular, lead candidate **16** combines high mGluR1 affinity, functional activity, selectivity versus mGluR5 as well as an improved water-solubility, which enables its use for in vivo investigations.

#### 4. Experimental

Melting points were determined in capillary tubes on a Gallenkamp melting point apparatus and are uncorrected. Microanalyses were performed on a Carlo Erba Instrument EA1108.  $^1\text{H}$  NMR spectra were recorded on Varian Mercury 200BB spectrometer for solutions in  $\text{CDCl}_3$  with TMS as internal standard. The solvents used were of commercial grade and were distilled before use. Flash chromatography was carried out on Kieselgel (35–70  $\mu\text{m}$ ). TLC analyses were performed on Kieselgel 60 F254 plates (Merck), UV-detection. Starting materials were from commercial sources.

##### 4.1. General procedure for the preparation of propenones

To a solution of aldehyde (**1** mmol) and methylketone (1.1 mmol) in ethanol (5 ml) was added 1 N NaOH (1.3 mmol). The mixture was stirred at room temperature for 1–13 days. The resulting precipitate was filtered off, washed with cold ethanol and dried under reduced pressure. If there were no precipitate the solution was evaporated under reduced pressure to dryness and purified by flash chromatography using a mixture of hexanes–EtOAc or  $\text{CH}_2\text{Cl}_2$ –MeOH as eluent.

##### 4.2. (*E*)-1-Cyclopropyl-3-quinolin-3-yl-propenone (**8**)

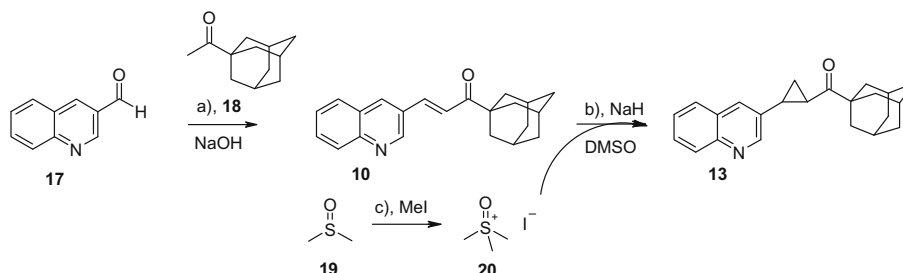
Yield 52%; mp 101–102 °C;  $R_f$  = 0.27 [hexane/EtOAc (2:1)];  $^1\text{H}$  NMR ( $\text{CDCl}_3$ )  $\delta$  1.04 and 1.22 (both m, both 2H,  $\text{CH}_2\text{CH}_2$ ); 2.30 (m, 1H, cyclopropyl CH); 7.11 (d, 16.2 Hz, 1H, =CH); 7.59 and 7.77 (both t, 7.4 and 6.6 Hz, both 1H, 6',7'-CH); 7.76 (d, 16.0 Hz, 1H, =CH); 7.86 and 8.12 (both d, 8.0 Hz, both 1H, 5',8'-CH); 8.29 (d, 2.2 Hz, 1H, 4'-CH) and 9.13 (d, 2.2 Hz, 1H, 2'-CH). Anal. Calcd for  $\text{C}_{15}\text{H}_{13}\text{NO}$ : C, 80.7; H, 5.9; N, 6.3. Found: C, 80.6; H, 5.8; N, 6.2.

##### 4.3. (*E*)-4,4-Dimethyl-1-quinolin-3-yl-pent-1-en-3-one (**9**)

Yield 45%; mp 146–148 °C;  $R_f$  = 0.34 [hexane/EtOAc (2:1)];  $^1\text{H}$  NMR ( $\text{CDCl}_3$ )  $\delta$  1.27 (s, 9H, 3 $\text{CH}_3$ ); 7.33 (d, 15.0 Hz, 1H, =CH); 7.59 and 7.76 (both t, 7.2 Hz, both 1H, 6',7'-CH); 7.83 (d, 15.2 Hz, 1H, =CH); 7.86 and 8.11 (both d, 7.8 and 8.0 Hz, both 1H, 5',8'-CH); 8.27 (d, 2.2 Hz, 1H, 4'-CH) and 9.13 (d, 2.2 Hz, 1H, 2'-CH). Anal. Calcd for  $\text{C}_{16}\text{H}_{17}\text{NO}\cdot 0.25\text{H}_2\text{O}$ : C, 78.8; H, 7.2; N, 5.7. Found: C, 78.5; H, 7.0; N, 5.7.

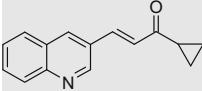
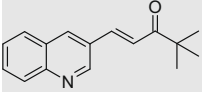
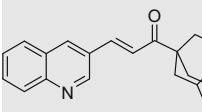
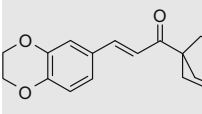
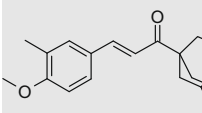
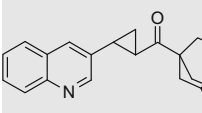
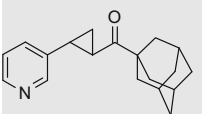
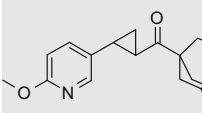
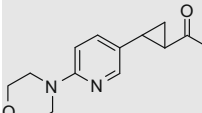
##### 4.4. (*E*)-1-Adamantan-1-yl-3-quinolin-3-yl-propenone (**10**)

Yield 69%; mp 169–171 °C;  $R_f$  = 0.34 [hexane/EtOAc (2:1)];  $^1\text{H}$  NMR ( $\text{CDCl}_3$ )  $\delta$  1.78 (s, 6H, adamantane  $\text{CH}_2$ ); 1.93 (s, 6H, adamantane  $\text{CH}_2$ ); 2.12 (br s, 3H, adamantane CH); 7.37 (d, 16.2 Hz, 1H, =CH); 7.58 and 7.75 (both t, 6.6 and 7.2 Hz, both 1H, 6',7'-CH); 7.83 (d, 16.2 Hz, 1H, =CH); 7.87 and 8.11 (both d, 8.2 Hz, both 1H, 5',8'-CH); 8.27 (d, 2.4 Hz, 1H, 4'-CH) and 9.13 (d, 2.2 Hz, 1H,



**Scheme 1.** Synthesis strategy for alkylpropenone (**8–12**) and cyclopropyl ketone derivatives (**13–16**). Reagents and conditions: (a) EtOH, aq NaOH (1 N), rt, 1–13 days, 29–88%; (b) NaH in DMSO, rt, 12 h, 70–90%; (c) MeI, 85 °C, 24 h, closed ampoule.

**Table 2**  
Structure and in vitro results for the alkylpropenone and cyclopropyl ketone derivatives

Chemical structure	ID	$K_i$ ( $\mu\text{M}$ ) rmGluR1	$K_i$ ( $\mu\text{M}$ ) rmGluR5	Selectivity $K_i$ (rmGluR5)/ $K_i$ (rmGluR1)
	<b>8</b>	>100	>100	–
	<b>9</b>	5.23 ( $\pm 0.98$ )	30.59	5.9
	<b>10</b>	0.021 ( $\pm 0.005$ )	0.807 ( $\pm 0.05$ )	29.9
	<b>11</b>	0.641 ( $\pm 0.05$ )	6.23 ( $\pm 0.72$ )	9.72
	<b>12</b>	0.294 ( $\pm 0.10$ )	5.15 ( $\pm 0.38$ )	17.51
	<b>13</b>	0.137 ( $\pm 0.05$ )	>100	>730
	<b>14</b>	7.04 ( $\pm 1.80$ )	22.94 ( $\pm 1.50$ )	3.26
	<b>15</b>	0.304 ( $\pm 0.02$ )	18.4 ( $\pm 0.63$ )	60.5
	<b>16*</b>	<b>0.024 (<math>\pm 0.001</math>)</b>	<b>27.78 (<math>\pm 0.38</math>)</b>	<b>1158</b>

Bold values highlight the high affinity of **16** for rmGluR1 and its selectivity versus rmGluR5.

\* hmGluR1 FLIPR – 0.11 + –0.02  $\mu\text{M}$  (repetitions:  $n = 4$ ).

2'-CH). Anal. Calcd for  $\text{C}_{22}\text{H}_{23}\text{NO} \cdot 0.25\text{H}_2\text{O}$ : C, 82.1; H, 7.4; N, 4.4. Found: C, 82.1; H, 7.3; N, 4.4.

#### 4.5. (E)-1-Adamantan-1-yl-3-(2,3-dihydro-benzo[1,4]dioxin-6-yl)-propenone (11)

Yield 29%; mp 125–127 °C;  $^1\text{H}$  NMR ( $\text{CDCl}_3$ )  $\delta$  1.75 (6H, s, adamantane  $\text{CH}_2$ ); 1.87 (d, 6H, adamantane  $\text{CH}_2$ ); 2.07 (s, 3H, adamantane CH); 4.28 (s, 4H,  $\text{CH}_2\text{CH}_2$ ); 6.85 (d, 8.0 Hz, 1H, 7'-CH); 7.00 (d, 1H, =CH); 7.09 (d, 8.0 Hz, 1H, 8'-CH); 7.11 (s, 1H, 5'-CH) and 7.56 (d, 15.2 Hz, 1H, =CH). Anal. Calcd for  $\text{C}_{21}\text{H}_{24}\text{O}_3$ : C, 77.7; H, 7.5. Found: C, 77.3; H, 7.6.

#### 4.6. (E)-1-Adamantan-1-yl-3-(4-methoxy-3-methyl-phenyl)-propenone (12)

Yield 41%; mp 138–140 °C;  $R_f = 0.53$  [hexane/EtOAc (4:1)];  $^1\text{H}$  NMR ( $\text{CDCl}_3$ )  $\delta$  1.76 (br s, 6H, adamantane  $\text{CH}_2$ ); 1.89 (br s, 6H, adamantane  $\text{CH}_2$ ), 2.09 (br s, 3H, adamantane CH); 2.24 (s, 3H,  $\text{CH}_3$ ); 3.86 (s, 3H,  $\text{OCH}_3$ ); 6.81 (d, 8.0 Hz, 1H, 5'-CH); 7.02 (d, 15.4 Hz, 1H, =CH); 7.38 (d, 8.0 Hz, 1H, 6'-CH); 7.40 (s, 1H, 2'-CH) and

7.59 ppm (d, 15.4 Hz, 1H, =CH). Anal. Calcd for  $\text{C}_{21}\text{H}_{26}\text{O}_2 \cdot 0.66\text{H}_2\text{O}$ : C, 78.3; H, 8.5. Found: C, 78.3; H, 8.5.

#### 4.7. General procedure for the preparation of cyclopropanones

By the method of Corey and Chaykovsky,<sup>32</sup> sodium hydride (60% dispersion in oil, 1.3 mmol) was added to a solution of trimethylsulfoxonium iodide (1.3 mmol) in DMSO (4 ml). After stirring for 15 min, propenone (1 mmol) solution in DMSO (2 ml) was added drop wise and it was stirred overnight. The reaction mixture was quenched with water (10 ml), extracted with methylene chloride ( $3 \times 10$  ml), dried ( $\text{MgSO}_4$ ) and evaporated under reduced pressure to give a crude product, which was purified by flash chromatography using a mixture of hexanes–EtOAc as eluent.

#### 4.8. Adamantan-1-yl-(2-quinolin-3-yl-cyclopropyl)-methanone hydrochloride (13)

Dry HCl solution in  $\text{Et}_2\text{O}$  was added, solvent was evaporated under reduced pressure, the residue was triturated with  $\text{Et}_2\text{O}$ , filtered and dried; yield 83%; mp 178–181 °C;  $^1\text{H}$  NMR ( $\text{CDCl}_3$ )  $\delta$

1.46–1.56 and 1.80–1.84 (both m, both 1H, cyclopropyl 3-CH<sub>2</sub>); 1.74 (s, 6H, adamantane CH<sub>2</sub>); 1.88 (s, 6H, adamantane CH<sub>2</sub>); 2.08 (s, 3H, adamantane CH); 2.56–2.73 (m, 2H, cyclopropyl 1,2-CH); 7.77 and 7.92 (both t, 8 Hz, both 1H, 6,7-CH); 7.96 (d, 9 Hz, 1H, 5-CH); 8.32 (s, 1H, 4-CH); 8.56 (d, 9 Hz, 1H, 8-CH) and 8.73 (d, 1.5 Hz, 1H, 2-CH). Anal. Calcd for C<sub>23</sub>H<sub>25</sub>NO·HCl·H<sub>2</sub>O: C, 71.6; H, 7.3; N, 3.6. Found: C, 71.7; H, 7.0; N, 3.6.

#### 4.9. Adamantan-1-yl-(2-pyridin-3-yl-cyclopropyl)-methanone hydrochloride (14)

Dry HCl solution in Et<sub>2</sub>O was added, solvent was evaporated under reduced pressure, the residue was triturated with Et<sub>2</sub>O, filtered and dried; yield 99%; mp 90–94 °C; <sup>1</sup>H NMR (CDCl<sub>3</sub>) δ 1.38–1.48 (m, 1H, cyclopropyl CH<sub>2</sub>); 1.66–1.80 (m overlapped by m, 7H, cyclopropyl CH<sub>2</sub>, adamantane CH<sub>2</sub>); 1.84–1.85 (m, 6H, adamantane CH<sub>2</sub>); 2.08 (s, 3H, adamantane CH); 2.56–2.64 (m, 2H, 2 cyclopropyl CH); 7.84 (dd, 8 and 8 Hz, 1H, 5-CH) 8.19 (d, 8 Hz, 1H, 4-CH); 8.47 (s, 1H, 2-CH) and 8.57–8.62 ppm (m, 1H, 1-CH). Anal. Calcd for C<sub>19</sub>H<sub>23</sub>NO·HCl·H<sub>2</sub>O: C, 68.0; H, 7.8; N, 4.2. Found: C, 68.7; H, 7.7; N, 4.1.

#### 4.10. Adamantan-1-yl-[2-(6-methoxy-pyridin-3-yl)-cyclopropyl]-methanone (15)

Yield 90%; mp 106–108 °C; <sup>1</sup>H NMR (CDCl<sub>3</sub>) δ 1.25 (td, 7.5 and 3.7 Hz, 1H, cyclopropyl-CH<sub>2</sub>); 1.54–1.63 (m, 1H, cyclopropyl-CH<sub>2</sub>); 1.64–1.73 (m, 6H, adamantane CH<sub>2</sub>); 1.85 (s, 6H, adamantane CH<sub>2</sub>); 2.05 (s, 3H, adamantane CH); 2.32 (t, 7 Hz, 2H, cyclopropyl CH); 3.91 (s, 3H, OCH<sub>3</sub>); 6.68 (d, 8 Hz, 1H, 5-CH); 7.29 (dd, 8 and 2 Hz, 1H, 4-CH) and 7.99 (d, 3 Hz, 1H, 2-CH). Anal. Calcd for C<sub>20</sub>H<sub>25</sub>NO<sub>2</sub>: C, 77.1; H, 8.1; N, 4.5. Found: C, 77.3; H, 8.3; N, 4.4.

#### 4.11. Adamantan-1-yl-[2-(6-morpholin-4-yl-2-pyridin-3-yl)-cyclopropyl]-methanone (16)

Yield 91%; mp 139–141 °C; *R*<sub>f</sub> = 0.33 [hexane/EtOAc (2:1)]; <sup>1</sup>H NMR (CDCl<sub>3</sub>) δ 1.20–1.27 (m, 1H, cyclopropyl CH<sub>2</sub>); 1.55–1.65 (m, 1H, cyclopropyl CH<sub>2</sub>); 1.64–1.82 (m, 6H, adamantane CH<sub>2</sub>); 1.86 (s, 6H, adamantane CH<sub>2</sub>); 2.05 (s, 3H, adamantane CH); 2.24–2.32 (m, 2H, cyclopropyl CH); 3.44–3.49 and 3.79–3.85 (both m, both 4H, morpholine NCH<sub>2</sub> and OCH<sub>2</sub>); 6.59 (d, 9 Hz, 1H, 5-CH); 7.25 (m overlapped by CHCl<sub>3</sub>, 1H, 4-CH) and 8.04 (d, 2 Hz, 1H, 2-CH). Anal. Calcd for C<sub>23</sub>H<sub>30</sub>N<sub>2</sub>O<sub>2</sub>: C, 75.4; H, 8.3; N, 7.6. Found: C, 75.2; H, 8.5; N, 7.6.

#### 4.12. mGluR1 binding assay—[<sup>3</sup>H]-2 assay

Cerebellar membranes were prepared according to Noeske et al.<sup>15</sup> On the day of assay the membranes were thawed and washed once more by re-suspension in 50 mM Tris-HCl, pH 7.5 and centrifugation at 48,000g for 20 min. The amount of protein in the final membrane preparation (250–500 µg/ml) was determined according to the method of Lowry et al.<sup>34</sup>

Binding assays were performed at room temperature in quadruplicate on 96-well format using fixed concentrations of test compound (10 µM). The assay was incubated for 1 h in the presence of 1 nM [<sup>3</sup>H]-2 and membranes (total volume 0.5 ml) and non-specific binding was estimated using 30 µM of the known mGluR1 antagonist (3-ethyl-2-methyl-quinolin-6-yl)-(4-hydroxy-cyclohexyl)-methanone.<sup>13</sup> Directly after transferring the reaction volume onto a 96-well multiscreen plate with glass fibre filter 0.22 µm (Millipore GmbH, Eschborn, Germany) binding was terminated by rapid filtration using a multiscreen vacuum manifold (Millipore GmbH, Eschborn, Germany). Afterwards, filters were washed three times with ice-cold assay-buffer and Ultima-Gold™

MV Scintillation Cocktail (Packard Bioscience, Groningen, The Netherlands) was added. After 14–16 h radioactivity was counted in a MicroBeta®Trilux (Perkin Elmer Life Sciences GmbH, Rodgau-Jügesheim, Germany).

#### 4.13. mGluR5 binding assay—[<sup>3</sup>H]MPEP assay

Cortical membranes were prepared according to Parsons et al.<sup>35</sup> Incubations were started by adding [<sup>3</sup>H]-MPEP (50.2 Ci/mmol, 5 nM, Tocris) to vials with 125–250 µg protein (total volume 0.5 ml) and various concentrations of the agents. The incubations were continued at room temperature for 60 min (equilibrium was achieved under the conditions used). Non-specific binding was defined by the addition of unlabelled MPEP (10 µM). Incubations were terminated using a Millipore filter system. The samples were rinsed twice with 4 ml of ice cold assay buffer over glass fibre filters (Schleicher & Schuell) under a constant vacuum. Following separation and rinse the filters were placed into scintillation liquid (5 ml Ultima Gold) and radioactivity retained on the filters was determined with a conventional liquid scintillation counter (Hewlett Packard, Liquid Scintillation Analyser).

#### 4.14. rmGluR1 assay for the determination of accumulation of [<sup>3</sup>H]-inositol phosphates

Cerebellar granule cells obtained from P8 postnatal Sprague Dawley rats were cultured in basal Eagle medium (BEM) supplemented with 10% foetal calf serum and 2 mM glutamine on 96 well plates—for further details see—Noeske et al. (2007). After 6 DIV the BEM was replaced completely with inositol free DMEM (MP Biomedicals, Eschwege, Germany) containing [<sup>3</sup>H]-myo-inositol (Perkin Elmer Life Sciences GmbH, Rodgau-Jügesheim, Germany) at a final concentration of 0.5 µCi/100 µl/well and incubated for a further 48 hours. The DMEM in each well was replaced with 100 µl Locke's buffer (plus 20 mM LiCl, pH 7.4) and incubated for 15 min at 37 °C. Locke's buffer was replaced with agonists/antagonists/putative mGluR1 ligands in Locke's buffer and incubated for 45 min. These solutions were then replaced with 100 µl 0.1 M HCl in each well and incubated for a further 10 min on ice in order to lyse the cells. The 96 well plates could be frozen at –20 °C at this stage until further analysis.

Home made resin exchange columns were prepared as follows. Empty Bio-Spin Chromatography columns (Biorad Laboratories GmbH, München, Germany) were plugged with filter paper before filling with 1.1–1.3 ml of resin (AG1-X8 Biorad, 140-14444) suspended in 0.1 M formic acid (24 g resin per 50 ml acid). The formic acid was allowed to run out before sealing the syringe tips and filling with 200–300 µl of 0.1 M formic acid before storage at 4 °C.

On the day of assay, columns were washed with 1 ml of 0.1 M formic acid followed by 1 ml of distilled water. Then the contents of each assay well were added to one column and washed with 1 ml distilled water followed by 1 ml of 5 mM sodium tetraborate/60 mM sodium formate. Thereafter, the retained radioactive inositol phosphates were eluted with 2 × 1 ml of 1 M ammonium formate/0.1 M formic acid into 24-well visiplates. Scintillation liquid (1.2 ml UltimaFlow AF, Perkin Elmer) was added to each well, the plate sealed and vortexed before radioactivity was determined by conventional liquid scintillation counting (MicroBeta®Trilux, Perkin Elmer Life Sciences GmbH, Rodgau-Jügesheim, Germany). Unless otherwise stated, all reagents were obtained from Sigma.

#### Acknowledgements

Tanja Bauer, Sabine Denk and Christina Wollenburg are thanked for technical assistance in performing functional mGluR1 assays

and mGluR5 binding assays. T.N. is grateful to Merz Pharmaceuticals GmbH for a PhD fellowship. This research was supported by the Beilstein-Institut zur Förderung der Chemischen Wissenschaften, Frankfurt am Main.

### Supplementary data

Supplementary data associated with this article can be found, in the online version, at doi:10.1016/j.bmc.2009.05.072.

### References and notes

- Wess, J. *Pharmacol. Ther.* **1998**, *80*, 231.
- Bockaert, J.; Pin, J. P. *Embo J.* **1999**, *18*, 1723.
- Lesage, A. S. *Curr. Neuropharmacol.* **2004**, *2*, 363.
- Kunishima, N.; Shimada, Y.; Tsuji, Y.; Sato, T.; Yamamoto, M.; Kumasaka, T.; Nakanishi, S.; Jingami, H.; Morikawa, K. *Nature* **2000**, *407*, 971.
- Pagano, A.; Ruegg, D.; Litschig, S.; Stoehr, N.; Stierlin, C.; Heinrich, M.; Floersheim, P.; Prezeau, L.; Carroll, F.; Pin, J. P.; Cambria, A.; Vranesic, I.; Flor, P. J.; Gasparini, F.; Kuhn, R. *J. Biol. Chem.* **2000**, *275*, 33750.
- Kew, J. N. *Pharmacol. Ther.* **2004**, *104*, 233.
- Williams, D. L., Jr.; Lindsley, C. W. *Curr. Top. Med. Chem.* **2005**, *5*, 825.
- Malherbe, P.; Kratochwil, N.; Mühlemann, A.; Zenner, M. T.; Fischer, C.; Stahl, M.; Gerber, P. R.; Jaeschke, G.; Porter, R. H. *J. Neurochem.* **2006**, *98*, 601.
- Gasparini, F.; Bilbe, G.; Gomez-Mancilla, B.; Spooren, W. *Curr. Opin. Drug Discov. Dev.* **2008**, *11*, 655.
- Belozertseva, I. V.; Kos, T.; Popik, P.; Danysz, W.; Bespalov, A. Y. *Eur. Neuropsychopharmacol.* **2007**, *17*, 172.
- Namkoong, J.; Martino, J. J.; Chen, S. *Front. Biosci.* **2006**, *11*, 2081.
- Zheng, G. Z.; Bhatia, P.; Daanen, J.; Kolasa, T.; Patel, M.; Latshaw, S.; Kouhen, O. F. E.; Chang, R.; Uchic, M. E.; Miller, L.; Nakane, M.; Lehto, S. G.; Honore, M. P.; Moreland, R. B.; Brioni, J. D.; Stewart, A. O. *J. Med. Chem.* **2005**, *48*, 7374.
- Mabire, D.; Coupa, S.; Adelinet, C.; Poncelet, A.; Simonnet, Y.; Venet, M.; Wouters, R.; Lesage, A. S.; Beijsterveldt, L. V.; Bischoff, F. *J. Med. Chem.* **2005**, *48*, 2134.
- Ito, S.; Satoh, A.; Nagatomi, Y.; Hirata, Y.; Suzuki, G.; Kimura, T.; Satow, A.; Maehara, S.; Hikichi, H.; Hata, M.; Kawamoto, H.; Ohta, H. *Bioorg. Med. Chem.* **2008**, *16*, 9817.
- Noeske, T.; Jirgensons, A.; Stachenkovs, I.; Renner, S.; Jaunzeme, I.; Trifanova, D.; Hechenberger, M.; Bauer, T.; Schneider, G.; Parsons, C. G.; Weil, T. *ChemMedChem* **2007**, *2*, 1763.
- Noeske, T.; Hechenberger, M.; Noeske, T.; Bocker, A.; Jatzke, C.; Schmuker, M.; Parsons, C. G.; Weil, T.; Schneider, G. *Angew. Chem., Int. Ed.* **2007**, *46*, 5336.
- Renner, S.; Noeske, T.; Parsons, C. G.; Schneider, P.; Weil, T.; Schneider, G. *ChemBioChem* **2005**, *6*, 620.
- Radestock, S.; Weil, T.; Renner, S. *J. Chem. Inf. Model.* **2008**, *48*, 1104.
- Bender, A.; Glen, R. C. *Org. Biomol. Chem.* **2004**, *2*, 3204.
- Vanejvs, M.; Jatzke, C.; Renner, S.; Müller, S.; Hechenberger, M.; Bauer, T.; Klochkova, A.; Pyatkin, I.; Kazyulkin, D.; Aksenova, E.; Shulepin, S.; Timonina, O.; Haasis, A.; Gutcaits, A.; Parsons, C. G.; Kauss, V.; Weil, T. *J. Med. Chem.* **2008**, *51*, 634.
- Gravius, A.; Pietraszek, M.; Schäfer, D.; Schmidt, W. J.; Danysz, W. *Behav. Pharmacol.* **2005**, *16*, 113.
- Kohonen, T. *Biol. Cybern.* **1982**, *43*, 59.
- Schneider, G.; Wrede, P. *Prog. Biophys. Mol. Biol.* **1998**, *70*, 175.
- Zupan, J.; Gasteiger, J. *Neural Networks in Chemistry and Drug Design*; Wiley-VCH: Weinheim, 1999.
- Noeske, T.; Sasse, B. C.; Stark, H.; Parsons, C. G.; Weil, T.; Schneider, G. *ChemMedChem* **2006**, *1*, 1066.
- Schneider, G.; Neidhart, W.; Giller, T.; Schmid, G. *Angew. Chem., Int. Ed.* **1999**, *38*, 2894.
- Schneider, G.; Schneider, P. *QSAR Comb. Sci.* **2003**, *22*, 713.
- Schneider, G.; Schneider, P. In *Drug Discovery*; Kubinyi, H., Müller, G., Eds.; Wiley-VCH: Weinheim, 2004; p 341.
- Ballesteros, J. A.; Weinstein, H. *Methods Neurosci.* **1995**, *25*.
- Malherbe, P.; Kratochwil, N.; Knoflach, F.; Zenner, M. T.; Kew, J. N.; Kratzenstein, C.; Maerki, H. P.; Adam, G.; Mutel, V. *J. Biol. Chem.* **2003**, *278*, 8340.
- Nielsen, A. T.; Houlihan, W. *J. Org. React.* **1968**, *16*, 1.
- Corey, E. J.; Chaykovsky, M. *J. Am. Chem. Soc.* **1962**, *84*, 867.
- Corey, E. J.; Chaykovsky, M. *J. Am. Chem. Soc.* **1965**, *87*, 1353.
- Lowry, O. H.; Rosebrough, N. J.; Farr, A. L.; Randall, R. J. *J. Biol. Chem.* **1951**, *193*, 256.
- Parsons, C. G.; Danysz, W.; Bartmann, A.; Spielmanns, P.; Frankiewicz, T.; Hesselink, M.; Eilbacher, B.; Quack, G. *Neuropharmacology* **1999**, *38*, 85.